Focusing of doughnut laser beams by a high numerical-aperture objective in free space

Djenan Ganic, Xiaosong Gan, and Min Gu

Centre for Micro-Photonics, School of Biophysical Sciences and Electrical Engineering
Swinburne University of Technology, P.O. Box 218, Hawthorn 3122, Australia
mgu@swin.edu.au

Abstract: We report on, in this letter, a phenomenon that the central zero-intensity point of a doughnut beam, caused by phase singularity, disappears in the focus, when such a beam is focused by a high numerical-aperture objective in free space. In addition, the focal shape of the doughnut beam of a given topological charge exhibits the increased ring intensity in the direction orthogonal to the incident polarization state and an elongation in the polarization direction. These phenomena are caused by the effect of depolarization, associated with a high numerical-aperture objective, and become pronounced by the use of a central obstruction in the objective aperture.

OCIS codes: (260.1960) Diffraction theory; (110.0180) Microscopy; (140.7010) Trapping

References and links

1. A. Ashkin, "Forces of a single-beam gradient laser trap on a dielectric sphere in the ray optics regime," Biophys. J. **61**, 569-581 (1992).
2. A. D. Mehta, M. Rief, J. A. Spudich, D. A. Smith, and R. M. Simmons, "Single-molecule biomechanics with optical methods," Science **283**, 1689-1695 (1999).
3. K. T. Gahagan and G. A. Swartzlander Jr., "Optical vortex trapping of particles," Opt. Lett. **21**, 827-829 (1996).
4. M. P. MacDonald, L. Paterson, K. Volke-Sepulveda, J. Arlt, W. Sibbett, K. Dholakia, "Creation and manipulation of three-dimensional optically trapped structures," Science, **296**, 1101-1103 (2002).
5. L. Paterson, M. P. MacDonald, J. Arlt, W. Sibbett, P. E. Bryant, and K. Dholakia, "Controlled rotation of optically trapped microscopic particles," Science **292**, 912-914 (2001).
6. M. Dyba and S. W. Hell, "Focal spots of size λ/23 open up far-field florescence microscopy at 33 nm axial resolution," Phys. Rev. Lett. **88**, 163901-1-4 (2002).
7. D. McGloin, V. Garcés-Chávez, and K. Dholakia, "Interfering Bessel beams for optical micromanipulation," Opt. Lett. **28**, 657-659 (2003).
8. M. W. Beijersbergen, R. P. C. Coerwinkel, M. Kristensen, and J. P. Woerdman, "Hellical-wavefront laser beam produced with a spiral phase plate," Opt. Commun. **112**, 321-327 (1994).
9. D. Ganic, X. Gan, and M. Gu, "Generation of doughnut laser beams by use of a liquid-crystal cell with a conversion efficiency near 100%," Opt. Lett. **27**, 1351-1353 (2002).
10. Y. Shin, K. Kim, J. A. Kim, H. R. Noh, W. Jhe, K. Oh, and U. C. Pack, "Diffraction-limited dark laser spot produced by a hollow optical fiber," Opt. Lett. **26**, 119-121 (2001).
11. N. R. Heckenberg, R. G. Mcduff, C. P. Smith, and A. G. White, "Generation of optical phase singularities by computer-generated holograms," Opt. Lett. **17**, 221-223 (1992).
12. M. Gu, *Advanced Optical Imaging Theory* (Springer, Heidelberg, 2000).
13. B. Richards, and E. Wolf, "Electromagnetic diffraction in optical systems, II. Structure of the image in an aplanatic system," Proc. Royal Soc. A. **253** (1959) 358-379.
14. J. W. M. Chon, X. Gan, and M. Gu, "Splitting of the focal spot of a high numerical-aperture objective in free space," Appl. Phys. Lett. **81**, 1576-1578 (2002).
15. H. C. Kim, and Y. H. Lee, "Hermite-Gaussian and Laguerre-Gaussian beams beyond the paraxial approximation," Opt. Commun. **169**, 9-16 (1999).
16. A. V. Volyar, V. G. Shvedov, and T. A. Fadeeva, "The structure of a nonparaxial Gaussian beam near the focus: II. Optical vortices," Opt. Spectrosc. **90**, 93-100 (2001).

#2826 - $15.00 US Received July 31, 2003; Revised October 14, 2003

1. Introduction

A TEM_{01}^{*} mode laser beam, also called a doughnut beam because of its characteristic shape, has been recently used in high-efficiency laser trapping [1-5] and super-resolution optical microscopy [6]. In particular, the use of a centrally obstructed doughnut beam focused by a high numerical-aperture (NA) objective facilitates the three-dimensional microstructure rotation with laser tweezers by extending its focal depth. Similar technique of focal depth extension has been demonstrated by using an axicon [7]. The electric field of a doughnut beam can be expressed as $E = E_0 \exp(in\varphi)$, where φ is the polar coordinate in the plane perpendicular to the beam axis and n is called the topological charge. Such a beam can be generated directly using a phase mask [8, 9] or a hollow optical fiber [10] or indirectly by using a computer-generated hologram [11].

It is well known that due to the helical phase distribution of a doughnut beam its intensity distribution gives zero on the axis, when it is focused by a low NA lens [12]. Physically, when a high NA lens is used the electric field in the focal region exhibits a component along the incident polarization direction as well as an orthogonal and a longitudinal component, which is called depolarization [12, 13]. The contribution of the longitudinal components is dependent on the phase and amplitude distribution on the lens aperture, which leads to the splitting of the focal spot of a ring beam [14]. Therefore, it could be expected that the focal intensity distribution of a doughnut beam focused by a high NA lens is different from that obtained using a low NA objective. Recent work on Laguerre-Gaussian beams in nonparaxial conditions indicates the presence of the longitudinal component of electric field, in addition to the transverse component [15,16]. However, it would be beneficial to quantify the strength of the longitudinal component for doughnut beams of different topological charges and focused by objectives of different NA.

In this letter we investigate the effect and strength of depolarization, induced by a high NA objective, on the focal intensity distribution of a doughnut beam.

2. Intensity distribution in the focal region

It is found that when a monochromatic doughnut beam, polarized in a transverse direction, is focused by a high NA objective in free space, the longitudinal component plays a significant role in determining the electric field in the focal region, resulting in the disappearing of the center zero intensity point.

Using the vectorial Debye theory, one can express the electric field distribution in the focal region of a linearly polarized monochromatic doughnut beam focused by a high NA objective satisfying the sine condition, if the polarization is along the x direction, as [12, 13]

$$\mathbf{E}(r_2,\psi,z_2) = \frac{i}{\lambda}\iint_{\Omega} \sqrt{\cos\theta}\exp(in\varphi)\exp[-ikr_2\sin\theta\cos(\varphi-\psi)]\exp(-ikz_2\cos\theta)$$

$$\{[\cos\theta+\sin^2\varphi(1-\cos\theta)]\boldsymbol{i}+\cos\varphi\sin\varphi(\cos\theta-1)\boldsymbol{j}+\cos\varphi\sin\theta\boldsymbol{k}\}$$

$$\sin\theta d\theta d\varphi \qquad (1)$$

where $\boldsymbol{i}$, $\boldsymbol{j}$, and $\boldsymbol{k}$ are unit vectors in the x, y, and z directions respectively. Variable r_2, ψ, and z_2 are the cylindrical coordinates of an observation point. Any other polarization state can be resolved in two orthogonal directions each of which satisfies Eq. (1).

The intensity is proportional to the modulus squared of Eq. (1) and is shown in Fig. 1 for doughnut beams of different topological charges and numerical aperture. When the numerical aperture of the focusing objective is low, the focal intensity distribution shows a well-known doughnut shape [12], which depends on topological charges. If, on the other hand, the numerical aperture of the focusing objective is high, the intensity distribution in the focal region becomes distorted and loses singularity for certain topological charges.

#2826 - $15.00 US Received July 31, 2003; Revised October 14, 2003

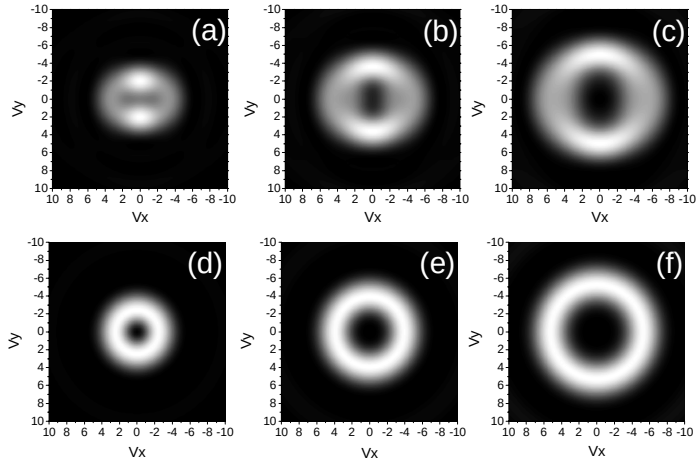

Fig. 1. Calculated intensity distribution in the focal region of a doughnut beam focused by an objective with NA=1 ((a)-(c)) and NA=0.2 ((d)-(f)): (a) and (d) Topological charge 1; (b) and (e) Topological charge 2; (c) and (f) Topological charge 3.

It can be seen from Fig. 1 that the intensity in the doughnut ring increases along the direction perpendicular to the incident polarization state and that the focal spot is elongated along the polarization direction. Furthermore, the doughnut beam of topological charges 1 and 2 (Figs. 1(a) and (b)) looses its zero intensity on the beam axis when focused by an objective of NA=1. For a beam of topological charge ±1, its intensity in the center of the focal region equals 48.8 % of the maximum intensity (Fig. 1(a)), while for a beam of topological charge ±2 it drops down to 13.5 % of the maximum intensity (Fig. 1(b)). When the topological charge becomes $-3 \geq n \geq 3$, the intensity in the center of the focal region regains its zero value (Fig. 1(c)). The zero intensity in the center of the focal region has been observed by calculating focal intensity distributions for higher doughnut beam topological charges (n=4 and n=5). This topological charge dependence of the intensity in the central focal region can be understood from Eq. (1).

Considering the point at the focus at $r = 0$ and $z = 0$, we find that $|E_x|^2 = 0$, $|E_y|^2 = 0$, and $|E_z|^2 \neq 0$ when $n = \pm 1$, because $\int_0^{2\pi} \cos(n\varphi)\cos(\varphi)d\varphi = 0$ for all n, except for $n = \pm 1$. In the case of $n = \pm 2$, the electric field components in the focal region give $|E_x|^2 \neq 0$, $|E_y|^2 \neq 0$, and $|E_z|^2 = 0$, because $\int_0^{2\pi} \cos(n\varphi)\sin^2\varphi d\varphi$ in the E_x component and $\int_0^{2\pi} \cos\varphi \sin\varphi \sin(n\varphi)d\varphi$ in the E_y component are non-zero for $n = \pm 2$. For $-3 \geq n \geq 3$, all integrals over φ give zero, which leads to the zero values of all the **E** field components at the center of the focal region.

A more detailed picture of the intensity $|\mathbf{E}|^2$ normalized to 100 and its components $|E_x|^2$, $|E_y|^2$ and $|E_z|^2$ near the focal region of an objective (NA=1) illuminated by a charge 1 doughnut beam polarized in the x direction is shown in Fig. 2. The contour plots are presented in terms of transverse optical coordinates V_x and V_y, which are defined as $V_{x,y} = k[x, y]\sin\alpha$, where k is the wave number and α is the maximum angle of convergence. It is evident that due to the high convergence angle, $|E_x|^2$ and $|E_z|^2$ components play a dominant role in

#2826 - $15.00 US Received July 31, 2003; Revised October 14, 2003

shaping the overall intensity $|\mathbf{E}|^2$. The high intensity of $|E_z|^2$ in the central region of the geometrical focus causes the non-zero value in the central region of the overall intensity distribution, and together with $|E_x|^2$ component leads to a "two-peak focus" in the V_y direction (Fig. 2(d)).

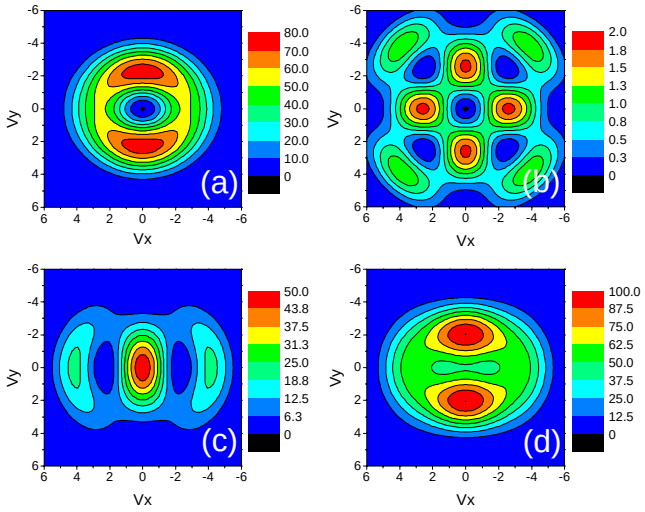

Fig. 2. Contour plots of the intensity distribution in the focal region of an objective with NA=1, illuminated by a doughnut beam of topological charge 1. (a) $|E_x|^2$; (b) $|E_y|^2$; (c) $|E_z|^2$; (d) $|\mathbf{E}|^2$.

Figure 3 gives the similar contour plots for a doughnut beam of topological charge 2. It is interesting to note that in this case $|E_y|^2$ component is comparable to $|E_x|^2$ in the central focal region, and that these two components result in the non-zero value in the center of the focal region. The central focal intensity for charge 2 is much smaller than that for charge 1. This is because the relative strength of $|E_z|^2$, which contributes to the central intensity for charge 1, is much larger than the relative strength of $|E_y|^2$. The combination of $|E_x|^2$ and $|E_z|^2$ components produces higher intensity peaks in the doughnut ring along the V_y direction (Fig. 3(d)).

The electric field components $|E_x|^2$, $|E_y|^2$ and $|E_z|^2$ all give zero field intensity in the central region of a doughnut beam of charge 3 (Fig. 4). Component $|E_x|^2$ gives a ring of equal intensity around the singularity (Fig. 4(a)), while component $|E_z|^2$ produces two high intensity peaks on either side of the singularity in the V_y direction (Fig. 4(c)). These two components are comparable in strength and are dominant in determining the overall intensity in the focal region.

#2826 - $15.00 US
Received July 31, 2003; Revised October 14, 2003

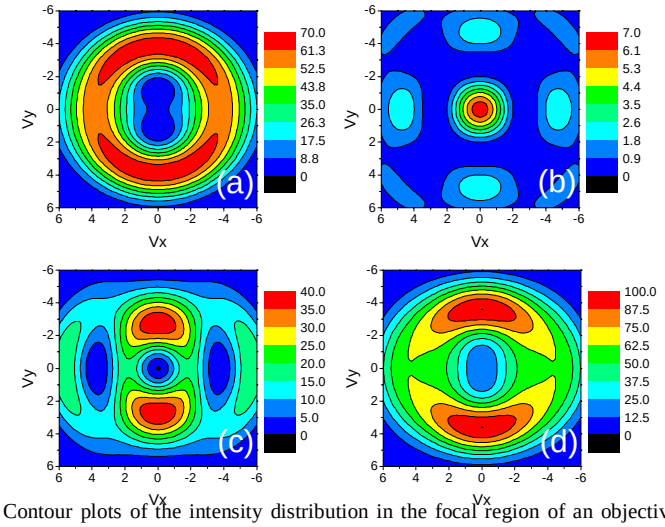

Fig. 3. Contour plots of the intensity distribution in the focal region of an objective with NA=1, illuminated by a doughnut beam of topological charge 2. (a) $|E_x|^2$; (b) $|E_y|^2$; (c) $|E_z|^2$; (d) $|\mathbf{E}|^2$.

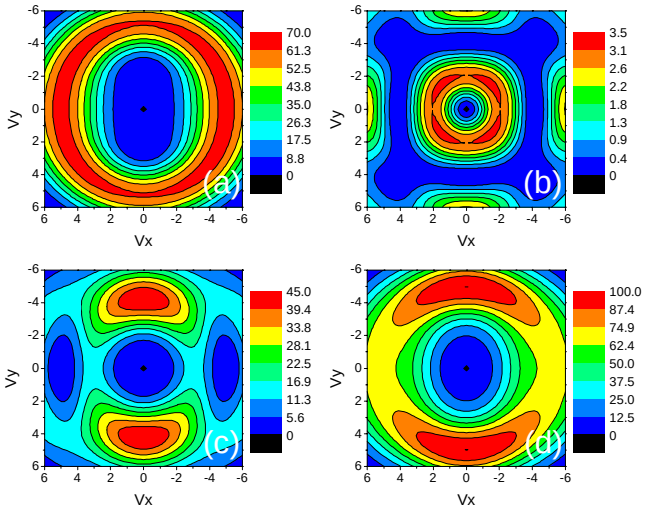

Fig. 4. Contour plots of the intensity distribution in the focal region of an objective with NA=1, illuminated by a doughnut beam of topological charge 3. (a) $|E_x|^2$; (b) $|E_y|^2$; (c) $|E_z|^2$; (d) $|\mathbf{E}|^2$.

3. Strength of longitudinal component

To investigate the relative strength of transversal $|E_x|^2$ and longitudinal $|E_z|^2$ field components, we have calculated the peak intensity ratio of $|E_z|^2/|E_x|^2$ as a function of NA for topological charges 1, 2 and 3 (Fig. 5(a)). It is seen that $|E_z|^2/|E_x|^2$ increases rapidly with NA. The longitudinal component $|E_z|^2$ of the doughnut beam attains approximately a half of the strength of the $|E_x|^2$ component even for NA=0.9. The increase is more rapid for topological

#2826 - $15.00 US
Received July 31, 2003; Revised October 14, 2003

charge 1 than that exhibited by the charges 2 and 3 beams of lower numerical aperture. As NA becomes larger, the most rapid increase is manifested by charge 3.

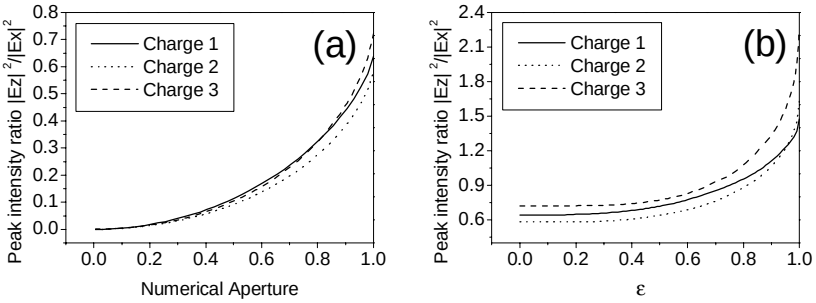

Fig. 5. Dependence of the peak ratio of $|E_z|^2/|E_x|^2$ on the numerical aperture (a) and on the obstruction radius ε (b).

Let us turn to the effect of a central opaque disk on the phenomenon shown in Figs. 1-4. Such centrally obstructed doughnut beam is analogous to using an axicon to extend the focal depth of the doughnut beam, which has been used in laser trapping with a high NA objective [7]. Figure 5(b) presents the dependence of the peak intensity ratio $|E_z|^2/|E_x|^2$ on the central obstruction ε for doughnut beams of charges 1, 2 and 3 for NA=1. Here, ε is defined as the ratio of the radius of the obstructed part to the radius of the unobstructed part of the beam. Presence of obstruction leads to more depolarized rays reaching the focus, which enhances the contribution from the $|E_z|^2$ component to the total intensity [12]. For example, for obstructions of $\varepsilon = 0.83$ and $\varepsilon = 0.87$ for a doughnut beam of charge 1 and charge 2, respectively, the longitudinal contribution equals the transverse one. For the limiting case of $\varepsilon \to 1.0$ the longitudinal contribution for the doughnut beam of charges 1, 2 and 3 is approximately 1.47, 1.64 and 2.25 times larger than that from the transverse component, respectively.

4. Conclusion

Focusing doughnut beams by a high NA objective in free space yields focal intensity distributions markedly different from those obtained when the same beam is focused by a low NA objective. The central zero intensity points disappear for doughnut beams of topological charges ±1 and ±2 due to the depolarization effect of a high NA objective. A doughnut beam of a given charge shows the increased ring intensity along the direction perpendicular to the incident polarization direction and that the focal spot becomes elongated in the polarization direction. These effects are more pronounced when such beams are centrally obstructed and may affect the performance of laser trapping [4, 5] and super-resolution optical microscopy [6], which involve focusing by a high NA objective.

Acknowledgments

The authors thank the Australian Research Council for its support.

#2826 - $15.00 US Received July 31, 2003; Revised October 14, 2003